The Astronomical Journal, 156:88 (13pp), 2018 September https://doi.org/10.3847/1538-3881/aad001

Magnetic Activity and Period Variation Studies of the Short-period Eclipsing Binaries. III. V1175 Her, NSVS 2669503, and 1SWASP J133417.80+394314.4

Hong-peng Lu[1], Raul Michel[2], Li-yun Zhang[1,3], and Angel Castro[2,4,5]
[1] College of Physics & Guizhou Provincial Key Laboratory of Public Big Data, Guizhou University, Guiyang 550025, People's Republic of China
liy_zhang@hotmail.com
[2] Observatorio Astronomico Nacional, Universidad Nacional Autonoma de Mexico, Apartado Postal 877, C.P. 22800 Ensenada, B.C., Mexico
[3] Key Laboratory for the Structure and Evolution of Celestial Objects, Chinese Academy of Sciences, Kunming 650011, People's Republic of China
[4] Physics and Astronomy, University of Southampton, Southampton SO17 1BJ, UK
Received 2017 November 11; revised 2018 June 21; accepted 2018 June 21; published 2018 August 9

Abstract

New multi-band CCD light curves of three binaries W UMa-type V1175 Her, NSVS 2669503, and 1SWASP J133417.80+394314.4 are presented. Spectroscopic data for V1175 Her and NSVS 2669503 show that their spectral types are G7V and K4V, respectively. Photometric solutions of these three objects were obtained with the help of the Wilson–Devinney program. We find that V1175 Her is a semi-detached binary star with a hot spot located on the secondary component, while NSVS 2669503 and 1SWASP J133417.80+394314.4 are contact eclipsing binaries with contact factors of $f = 1.070 \pm 0.002\%$ and $f = 21.250 \pm 0.005\%$, respectively. Moreover, we found that the orbital period of V1175 Her is increasing at a rate of $(+3.1 \pm 0.1) \times 10^{-7}$ days yr^{-1}. This increase may be attributed to a $dM_1/dt = -0.93 \times 10^{-7} M_\odot$ yr^{-1} mass-transfer rate from the primary to the secondary component. Finally, we discuss the evolutionary stage of the component stars of these three systems.

Key words: binaries: eclipsing – stars: activity

Supporting material: data behind figure

1. Introduction

W UMa-type stars are a special class of short-period oscillation and low-temperature eclipsing binaries (Binnendijk 1965, 1970). These binary systems are generally composed of two main-sequence A–K spectral type stars whose temperatures are very similar due to the efficient heat transfer through their convective common envelope (Lucy 1968a, 1968b). A common feature among light curves (LCs) of W UMa stars is the fact that the depths of their minima are nearly equal. The maxima are not always symmetrical due to the O'Connell effect (O'Connell 1951), namely an asymmetry of the out-of-eclipse brightness maxima of some eclipsing binaries, which may be caused by starspot on the components of the eclipsing binaries. There are two subclasses of W UMa binaries: type-A and type-W binaries (Binnendijk 1970). In type-A binaries, the more massive component is larger and hotter, whereas in type-W binaries, the more massive component is larger but cooler than its partner. Although both types of W UMa binaries may show the O'Connell effect, type-W tend to show more of this behavior (Davidge & Milone 1984; Kallrath & Milone 1999).

W UMa stars are in the most extreme and least understood stages of eclipsing binary interaction and evolution. The evolution of these kinds of system depends on both their initial mass and chemical composition. However, in spite of the recent advances in the field, there is still a lack of precise mass determination of W UMa stars found in the literature. The use of precise values of mass, luminosity, and other physical parameters plays an important role in the testing of different models of structure and stellar evolution (Kallrath & Milone 1999). This makes W UMa stars particularly valuable subjects for both spectroscopic and photometric studies. Such spectroscopic studies include the use of emission lines formed in the chromosphere as an index of chromospheric activity. In the optical band, the main chromospheric activity indicators are Hα (6562.8 Å) line, Hβ (4860.7 Å), Hγ (4340.1 Å), Hδ (4101.2 Å), Ca II H (3968 Å) and K (3933 Å), and Ca II IRT (8498, 8542, 8662 Å) emission lines in the spectrum (Wilson 1978; Hall 2008; Richards et al. 2014; Butler et al. 2015; Zhang et al. 2017). Since W UMa stars typically have short orbital periods, they often require few photometric observations to be able to obtain all-phase LCs from which absolute stellar parameters can be estimated using the Wilson–Devinney (WD) program (Wilson & Devinney 1971; Wilson 1979, 1990, 1994; R. E. Wilson & W. van Hamme 2004, private communication). The WD is a widely accepted tool in assessing the photometric solutions of eclipsing binaries (see Section 4 for more details).

V1175 Her ($\alpha(2000) = 16^h24^m46^s.22$, $\delta(2000) = +21°39'03''.3$) is an EW-type eclipsing binary system first reported by Akerlof et al. (2000) based on ROTSE-I observations. Blättler & Diethelm (2007) performed full phase *R*- and *V*-band CCD photometric observations of V1175 with an SBIG St-7 camera attached to a 15 cm Starfire refractor telescope in Wald, Switzerland during eight nights between JD2453858 and JD 2453910. The authors estimated its stellar parameters and provided linear ephemeris: JD (min I, hel) = 2453900.5264 +0.321156 × *E*. The system NSVS 2669503 ($\alpha(2000) = 12^h50^m17^s.40$, $\delta(2000) = +52°31'35''.1$) was also reported by Akerlof et al. (2000), while Woźniak et al. (2004) included it in the Northern Sky Variability Survey. Hoffman et al. (2009) classified NSVS 2669503 as a W UMa candidate and estimated

[5] Royal Astronomical Society, Newton International Fellow.

Table 1
Previously Known Fundamental Parameters of the Three Short-period W UMa Binaries

Object	P (days)	M[a] (mag)	A[b] (mag)	Primary Depth (mag)	Secondary Depth (mag)	Filter[c]	$(J–H)$[d] (mag)	$(J–K_S)$[d] (mag)	References
(1)	(2)	(3)	(4)	(5)	(6)	(7)	(8)	(9)	(10)
V1175 Her	0.32118699	11.320	0.278	0.18	0.15	R	⋯	⋯	(1) & (2)
NSVS 2669503	0.234004	13.494	0.404	⋯	⋯	⋯	0.599	0.100	(3) & (4)
J1334	0.228882	14.62	0.34	0.15	0.17	V	⋯	⋯	(5) & (6)

Notes.
[a] Magnitude derived from unfiltered photometry.
[b] Signal amplitude derived from unfiltered photometry.
[c] The filter used for primary and secondary optical depths determination.
[d] $(J–H)$ and $(J–K_S)$ magnitudes of the combined photometry of the eclipsing binary system.
References. (1) Akerlof et al. (2000), (2) Blättler & Diethelm (2007), (3) Hoffman et al. (2009), (4) Drake et al. (2014), (5) Lohr et al. (2013), (6) Palaversa et al. (2013).

its preliminary stellar parameters. After that, NSVS 2669503 was also included in the Catalina Sky Survey (CSS; Larson et al. 2003) and its photometric data were presented in CSS-DR1 (Drake et al. 2012). Using the CSS-DR1 photometric data, Drake et al. (2014) confirmed that NSVS 2669503 was an EW-type eclipsing binary system with a period of $0^{\rm d}.234004$. The system 1SWASP J133417.80+394314.4 ($\alpha(2000) = 13^{\rm h}34^{\rm m}17^{\rm s}.80$, $\delta(2000) = +39°43'14''.3$; hereafter J1334) was observed by the Wide Angle Search for Planets (SuperWASP) project (Pollacco et al. 2006; Lohr et al. 2013). By analyzing photometric data the authors derived its preliminary stellar parameters. In addition, J1334 was also included in the Lincoln Near-Earth Asteroid Research (LINEAR) asteroid survey (Sesar et al. 2011). Palaversa et al. (2013) investigated this object and argue that it was an EW-type eclipsing binary star. Previously known fundamental parameters of the three short-period W UMa binaries are listed in Table 1.

This paper is one of a series of published papers on the magnetic activity and orbital period variations of short-period eclipsing binaries (e.g., Pi et al. 2014, 2017). We present new full phase multi-band CCD photometric LCs of three objects and spectra of two (V1175 Her and NSVS 2669503). Using these data, we discuss the orbital and spot parameters, as well as spectral types each. Multi-band photometric and spectroscopic observations are presented in Section 2. Updates on linear ephemeris and orbital period analysis are described in Section 3. In Section 4 we used the 2003 version of the WD program in order to calculate their photometric solutions. In Section 5, we present the spectral types of V1175 Her and NSVS 2669503 as G7V (±2 subtypes) and K4V (±2 subtypes), respectively. Photometric solutions are discussed in Section 6. Our results suggest that V1175 Her is a semi-detached binary system with a hot spot on its secondary component and that its orbital period is increasing due to a mass-transfer effect. Both, NSVS 2669503 and J1334, are contact eclipsing binaries. A hot spot was found on the secondary component of NSVS 2669503. In addition, we derived the absolute parameters of the three systems. Finally, we found that the primary components of V1175 Her and J1334 are main-sequence (MS) stars. The primary component of NSVS 2669503 is an evolved MS star. The secondary components of V1175 Her and J1334 are sub-giants, while the secondary component of NSVS 2669503 is an M5 type dwarf star with a mass of 0.21 $M_\odot$.

2. Photometric and Spectroscopic Observations

Photometric CCD data were acquired at the OAN-SPM[6] observatory in Baja California, Mexico. All images were processed with IRAF.[7] Several flat-fields for each of the filters were obtained each night by observing at twilight a "clear of stars" sky-patch towards the anti-Sun direction. Standard bias, flat-field, and cosmic-ray removal[8] correction procedures were applied. The instrumental magnitudes of the binary, comparison, and check stars were measured utilizing the standard aperture photometry packages of IRAF. The aperture used, for each observing set, was defined as 1.5 times the average FWHM (full width at half maximum) for each image. This assured that close to 100% of the light was collected and that the effect of nearby stars was reduced.

V1175 Her was observed on 2016 June 1 using the 2.12 m telescope, in its $f/13.5$ configuration. The telescope was equipped with a filter wheel and the Marconi-4 CCD detector with a field of view of $3'.3 \times 3'.3$. Alternated U, B, V, R and I_C-band images were taken, with exposure times of 60, 15, 6, 3, and 3 s, respectively, for a total of 7.7 hr. After calibrating the field stars using Landolt equatorial standard stars (Landolt 1992, 2009), it was found that TYC1518-849-1 (2MASS J16244549+2135527) was a good comparison star since it has similar color indexes to V1175 Her. Its measured relative magnitudes are $U = 12.585$, $B = 12.270$, $V = 11.533$, $R = 11.105$ and $I_C = 10.753$. According to the 2MASS All-Sky Point Source Catalog[9] (Skrutskie et al. 2006), their infrared magnitudes are $J = 10.173$, $H = 9.838$ and $K_S = 9.773$ mag. 2MASS J16245618+2136053 ($J = 11.358$, $H = 11.117$, $K_S = 11.071$ mag) was selected as check star. The magnitude difference between the comparison star and check star is stable within 0.02 mag in *UBVRI* bands.

Observations for NSVS 2669503 and J1334 were carried out with the 0.84 m telescope using the MEXMAN filter wheel and the Marconi-3 detector and a field of view of $7'.6 \times 7'.6$. NSVS 2669503 was observed during two nights. Alternated B, V, and R images were taken on 2016 March 22, with corresponding

[6] Observatorio Astronómico Nacional, Sierra de San Pedro Mártir (http://www.astrossp.unam.mx/oanspm/index.php).
[7] IRAF (http://iraf.noao.edu/) is distributed by the National Optical Astronomy Observatories, which are operated by the Association of Universities for Research in Astronomy, Inc., under cooperative agreement with the National Science Foundation.
[8] L.A.Cosmic (http://www.astro.yale.edu/dokkum/lacosmic).
[9] https://www.ipac.caltech.edu/2mass/releases/allsky/

exposure times of 80, 35, and 20 s, for a total of 5.9 hr. On 2016 March 26, the $UBVRI_C$ filters were used, with exposure times of 500, 120, 60, 50, and 50 s, respectively, for a total of 6.3 hr. The field stars were also calibrated and 2MASS J12502674+5233221 ($U = 15.391$, $B = 15.269$, $V = 14.563$, $R = 14.156$, $I_C = 13.752$, $J = 13.252$, $H = 12.862$, and $K_S = 12.752$) and 2MASS J12500559+5231242 ($J = 13.354$, $H = 12.743$, $K_S = 12.574$ mag) were chosen as comparison and check star, respectively. The magnitude difference between them is stable within 0.02 mag in *UBVRI* bands. J1334 was observed on 2016 April 25, in the *B*, *V* and *R* optical bands, with exposure times of 30, 15 and 10 s, respectively, for a total of 8.1 hr. 2MASS J13341518+3940592 ($U = 15.725$, $B = 15.664$, $V = 15.048$, $R = 14.691$, $I_C = 14.355$, $J = 13.870$, $H = 13.532$, $K_S = 13.505$ mag) and 2MASS J13342182+3940205 ($J = 12.963$, $H = 12.677$, $K_S = 12.623$ mag) were chosen as comparison star and check star, and the magnitude difference between them is also stable within 0.08 mag in *BVR* bands.

After standard aperture photometry, we obtained the full phase LCs of the described systems and the corresponding magnitude difference between the comparison star and check star in each band (see Figure 1). From the Figure 1, it can be seen that the magnitude difference between the comparison star and check star in each band are stable and they are much smaller than the LCs' trends of the three eclipsing binaries. In addition, it can be seen that the LCs of V1175 Her display the O'Connell effect with the height at phase 0.25 being higher than that at phase 0.75. The LCs of NSVS 2669503 also show the O'Connell effect, with the secondary maxima of the LCs being a little higher than the primary ones.

Spectroscopic data of V1175 Her was obtained on 2017 February 09 using the Yunnan Faint Object Spectrograph and Camera (YFOSC; Fan et al. 2015) instrument of the Lijiang 2.4 m telescope in Yunnan Astronomical Observatory,[10] China. We used a long slit width of 2.″5 and low-resolution Grism 3, which provides a resolution of 172 Å/mm covering the 3200–9200 Å wavelength range. Bias subtraction, flat-field calibration, cosmic-ray removal, spectral extraction, sky subtraction, wavelength calibration and wavelength band combination were performed with IRAF. The spectrum of V1175 Her is plotted in the left panel of Figure 2.

Spectroscopic data of NSVS 2669503 was obtained using the Large Sky Area Multi-Object Fibre Spectroscopic Telescope survey (LAMOST[11]; Wang et al. 1996; Luo et al. 2012; Zhang et al. 2018) on 2013 February 15. LAMOST is located in Xinglong Station of the National Astronomical Observatory, Chinese Academy of Sciences (NAOC). This telescope is equipped with 4000 fibers and a resolution $R \sim 1800$ (Cui et al. 2012; Zhao et al. 2012). The LAMOST Data Release 3 (DR3)[12] includes 5755126 spectra with wavelength range of about $3700 < \lambda[\text{Å}] < 9100$. The downloaded spectrum of NSVS 2669503 was reduced using the LAMOST two-dimensional pipeline. The spectrum of NSVS 2669503 is shown in the right panel of Figure 2.

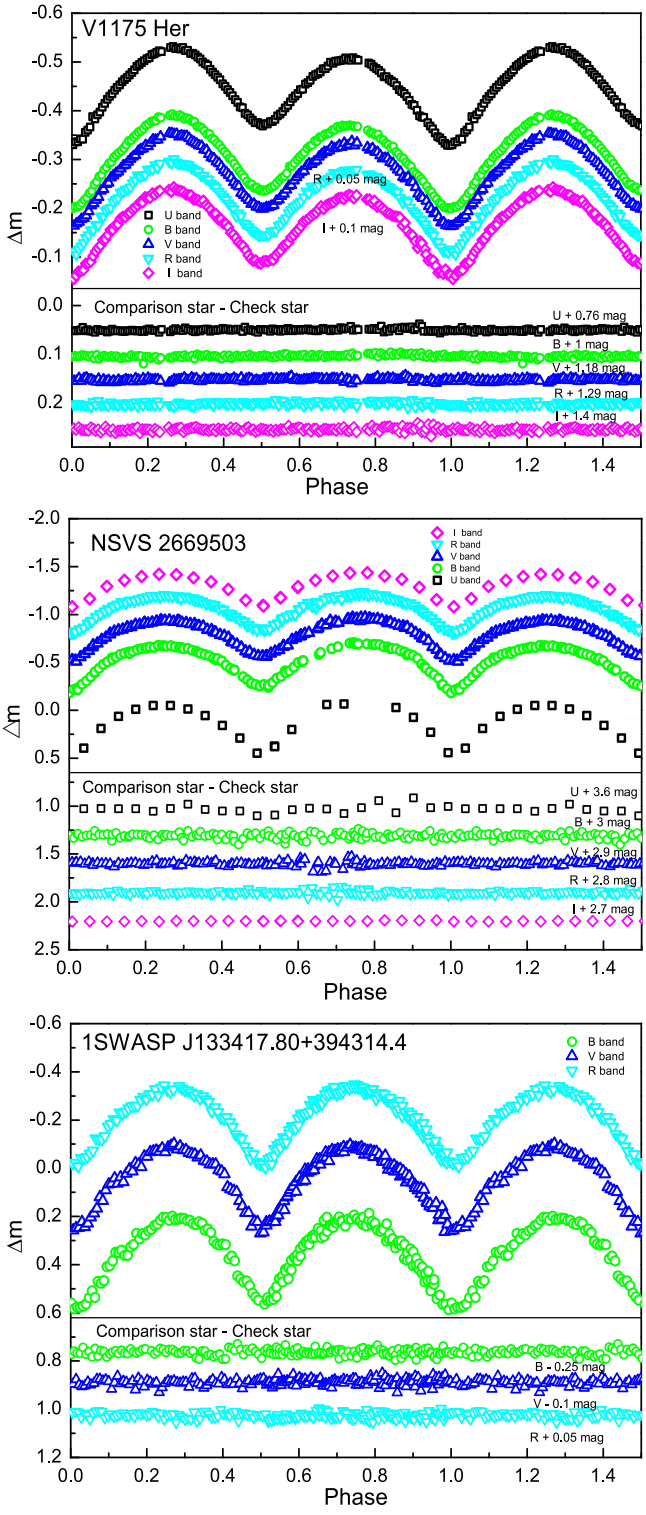

Figure 1. Multi-band observed LCs of the three eclipsing binary stars according to the phase. V1175 Her was observed on 2016 June 01. NSVS 2669503 was observed on 2016 March 22 and 26. J1334 was observed on 2016 March 22 and 26. The magnitude difference between the comparison star and check star in each band are shown in the down panel of each LCs. The multi-band photometry shown in this figure is available as the Data behind the Figure. The data used to create this figure are available.

3. Ephemeris and Period Analysis

New light minimum times are of great importance to deduce linear ephemeris and analyze periodic variations of eclipsing binary systems. In order to obtain the light minimum times for each band, we fitted the LCs of the three eclipsing binaries with the program of Nelson (2007) using the method described

[10] http://english.ynao.cas.cn/
[11] http://www.lamost.org
[12] http://dr3.lamost.org/

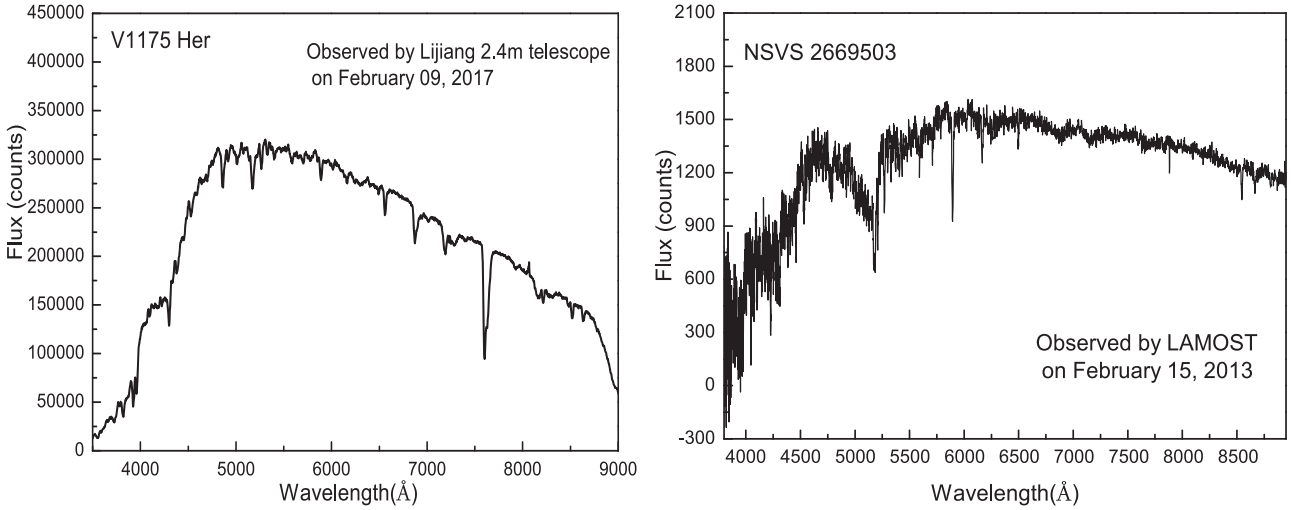

Figure 2. Spectroscopic observations of V1175 Her and NSVS 2669503. The vertical axis in the figure represents the relative flux.

Table 2
New Light Minimum Times of V1175 Her, NSVS 2669503, and J1334

Object (1)	HJD (2)	Uncertainty (3)	Type (4)
V1175 Her	2457540.69435	0.00015	Primary
	2457540.85718	0.00011	Secondary
NSVS 2669503	2457469.86506	0.00147	Primary
	2457469.98108	0.00157	Secondary
	2457473.84342	0.00524	Primary
	2457473.95904	0.00610	Secondary
J1334	2457503.79057	0.00120	Primary
	2457503.90426	0.00187	Secondary

in Kwee & van Woerden (1956). The resultant light minimum times of our three objects are the averages of the light minimum times in the observed bands. The corresponding minimum times, their uncertainties and the type of minimum times are listed in Table 2.

For V1175 Her, we gathered all the available data on light minimum times from the Eclipsing Binaries Minima Database[13] (Paschke & Brát 2006) and from the literature. There are 17 light minimum times of V1175 Her reported in literature and 2 light minimum times observed by us. These minima are listed in Table 3; column 1 is the HJD of light minimum times; column 2 is their uncertainty; column 3 is epoch, calculated from the previous ephemeris JD(min, hel) = 2453900.5264 +0.321156 × E (Blättler & Diethelm 2007); column 4 is the type of light minimum time and column 5 shows the method employed to determine the light minimum time. By fitting the epoch versus HJD of Table 3 with a straight line, we estimated the following linear ephemeris:

$$\begin{aligned}\mathrm{Min.I} = {} & \mathrm{HJD}2453900.526195(\pm 0.000002) \\ & + 0^{\mathrm{d}}.32120004(\pm 0.00000008)E, \end{aligned} \quad (1)$$

where E represents the epoch. The parameter O–C is defined as the difference between the minimum time of observation and the calculation. The corresponding values of the linear fitting residuals $(O-C)_{\mathrm{I}}$ (see Equation (1)) are shown in the sixth column of Table 3. In order to study the period variation, we plotted the $(O-C)_{\mathrm{I}}$ versus E in Figure 3, which shows an obvious upward parabolic trend. Therefore, we used a quadratic curve to fit this trend. The resultant quadratic ephemeris is:

$$\begin{aligned}\mathrm{Min.I} = {} & \mathrm{HJD}2453900.528975 \pm 0.000006 \\ & + 0^{\mathrm{d}}.32119581(\pm 0.00000004)E \\ & + 4.21(\pm 0.08) \times 10^{-10}E^2. \end{aligned} \quad (2)$$

Quadratic fitting residuals $(O-C)_{\mathrm{II}}$ are given in Table 3 (column 7). The quadratic term (Q) of this equation was found to be $+4.21(\pm 0.08) \times 10^{-10}$, suggesting that the orbital period variation is increasing by a rate of $dP/dt = +3.1(\pm 0.1) \times 10^{-7}$ days yr^{-1}.

For NSVS 2669503 and J1334, there is no other light minima available in literature for comparison. Here we just fitted our minimum light times with a straight line. The linear ephemeris of NSVS 2669503 is:

$$\begin{aligned}\mathrm{Min.I} = {} & \mathrm{HJD}2457469.864585(\pm 0.000006) \\ & + 0^{\mathrm{d}}.23400736(\pm 0.00000003)E. \end{aligned} \quad (3)$$

Our calculated period is 0.23400736 days, which is very similar to the 0.234004-days value reported by Drake et al. (2014). The linear ephemeris of J1334 is:

$$\begin{aligned}\mathrm{Min.I} = {} & \mathrm{HJD}2457503.790569(\pm 0.000005) \\ & + 0^{\mathrm{d}}.22738000(\pm 0.00000003)E. \end{aligned} \quad (4)$$

From the above equation, the period is 0.22738000 days, which is a little lower than the 0.228882-days period estimated by Palaversa et al. (2013).

4. Orbital Parameters

Geometric and photometric parameters of the systems were derived using the WD program. These parameters can be computed from monochromatic LCs of the eclipsing binary stars. To do this, WD calls the synthetic LC and Differential Correction (DC) subroutines. LC is used to generate LCs and radial velocity curves. DC is used to obtain the best-fitting solutions of light and velocity curves using the technique of

[13] http://www.oa.uj.edu.pl/ktt/index.html

Table 3
V1175 Her Light Minimum Times Fitting Parameters

HJD(2400000,+) (1)	Uncertainty (2)	Epoch (3)	Type (4)	$(O-C)_{\rm I}$ (5)	$(O-C)_{\rm II}$ (6)	References (7)
53858.45690	0.00180	−131	Primary	0.0079	0.0046	(1)
53877.40430	0.00170	−72	Primary	0.0045	0.0014	(1)
53894.58300	0.00300	−18.5	Secondary	−0.0010	−0.0039	(1)
53896.50960	0.00080	−12.5	Secondary	−0.0016	−0.0044	(1)
53898.43820	0.00090	−6.5	Secondary	−0.0002	−0.0030	(1)
53900.52670	0.00070	0	Primary	0.0005	−0.0023	(1)
53906.46780	0.00060	18.5	Secondary	−0.0006	−0.0033	(1)
53910.48370	0.00040	31	Primary	0.0003	−0.0023	(1)
54295.44690	0.00070	1229.5	Secondary	0.0053	0.0070	(2)
54318.41420	0.00100	1301	Primary	0.0067	0.0088	(2)
54916.80180	0.00050	3164	Primary	−0.0013	0.0051	(3)
55049.45170	0.00090	3577	Primary	−0.0070	−0.0001	(4)
56038.42250	0.00210	6656	Primary	−0.0112	−0.0045	(5)
56038.58450	0.00130	6656.5	Secondary	−0.0098	−0.0031	(5)
56051.43338	0.00090	6696.5	Secondary	−0.0089	−0.0022	(5)
56135.42746	0.00020	6958	Primary	−0.0086	−0.0023	(6)
57120.88440	0.00040	10026	Primary	0.0066	0.0039	(7)
57540.69435	0.00015	11333	Primary	0.0081	−0.0008	(8)
57540.85718	0.00011	11333.5	Secondary	0.0103	0.0014	(8)

References. (1) Diethelm (2007), (2) Diethelm (2008), (3) Nelson (2010), (4) Diethelm (2010), (5) Banfi et al. (2012), (5) Hoňková et al. (2013), (1) Nelson (2016), (8) This paper.

least squares. WD also allows us to consider important parameters such as rotational and tidal distortion, the reflection effect, limb-darkening and gravity-darkening, among others. With WD, photometric data can be fitted using different models included in the code (detached, semi-detached, overcontact and double contact), to obtain the fundamental physical parameters, such as inclination, monochromatic luminosity ratio, temperature, mass ratio and surface potential.

All of our CCD photometric LCs have full phase coverage and high time resolution measurements. This allowed us to use the WD program in order to obtain photometric solutions of the studied eclipsing binary stars. The selection of the correct model is of great importance when running the WD program. Since V1175 Her was previously classified as an EW-type by Akerlof et al. (2000), we first tried Mode 3 (contact binary) to obtain a solution. However, our result showed that V1175 Her is not a contact binary. We adopted Mode 4 (semi-contact binary) for calculations. Since NSVS 2669503 is a W UMa-type eclipsing binary star (Drake et al. 2014) and J1334 is also an EW-type eclipsing binary star (Palaversa et al. 2013), we chose Mode 3 (contact binary) to calculate the photometric solutions for these two systems.

Before calculations, some initial parameters for each star had to be provided as a set of inputs to WD program. One of these parameters is the effective temperature ($T_{\rm eff}$) of the primary component. Here, we used the equation

$$T_{\rm eff} = -4369.5 \times (J - H) + 7188.2; \quad \text{for } 4000 < T_{\rm eff}\,[\rm K] < 7000, \tag{5}$$

proposed by Collier et al. (2007) to deduce the temperature. The J and H magnitude values and their uncertainties were taken from the 2MASS All-Sky Catalog. The estimated $T_{\rm eff}$ of the primary component of V1175 Her, NSVS 2669503 and J1334 are 5362 ± 224 K, 4571 ± 176 K and 4872 ± 155 K, respectively. The bolometric albedo of both the primary and secondary components of our three objects were set to $A_1 = A_2 = 0.5$ (Rucinski 1973) and their gravity-darkening (g) coefficients were set to $g_1 = g_2 = 0.32$ (Lucy 1967). For V1175 Her, the bolometric limb-darkening coefficient (x) of the primary component is $x_{\rm 1bolo} = 0.526$; the limb-darkening coefficients of the primary component for the $UBVRI_{\rm C}$ bands are $x_{1U} = 0.923$, $x_{1B} = 0.804$, $x_{1\rm V} = 0.666$, $x_{1R} = 0.551$ and $x_{1I} = 0.452$, respectively (Van Hamme 1993) . For NSVS 2669503, the bolometric limb-darkening coefficient and the limb-darkening coefficients for $UBVRI_{\rm C}$ bands of the primary component are $x_{\rm 1bolo} = 0.534$, $x_{1U} = 1.058$, $x_{1B} = 0.804$, $x_{1V} = 0.666$, $x_{1R} = 0.551$ and $x_{1I} = 0.452$, respectively. For J1334, the corresponding coefficients of the primary component are $x_{\rm 1bolo} = 0.538$, $x_{1B} = 0.886$, $x_{1V} = 0.744$, $x_{1R} = 0.614$, respectively. Once these parameters were obtained, we could run the WD program in order to obtain the photometric solutions. When setting Mode 3 (contact binary) and Mode 4 (semi-contact binary) in the WD program, the adjustable parameters are the mass ratio ($q = M_2/M_1$), the orbital inclination (i), the secondary component temperature (T_2), the dimensionless potentials (Ω) and the monochromatic luminosities of the primary component (L_{1U}, L_{1B}, L_{1V}, L_{1R} and L_{1I}). Moreover, for V1175 Her and NSVS 2669503, we also need to adjust the spot parameters, including latitude (we assumed an equatorial location of the spot), longitude, angular radius and temperature factor.

A precise mass ratio, q, is mandatory in order to obtain an accurate photometric solution. In this paper, we use the LCs fitting residuals Σ versus q to estimate these mass ratios. For NSVS 2669503 and J1334, we plotted the fitting residuals Σ–q relations in Figure 4. This indicates that the most likely mass ratio is 0.3 and 5.4 for NSVS 2669503 and J1334, respectively. For V1175 Her, however, due to the asymmetry of the LC, the fitting residuals decrease as the mass ratio increases. From the above period oscillation analysis, we known that the orbital

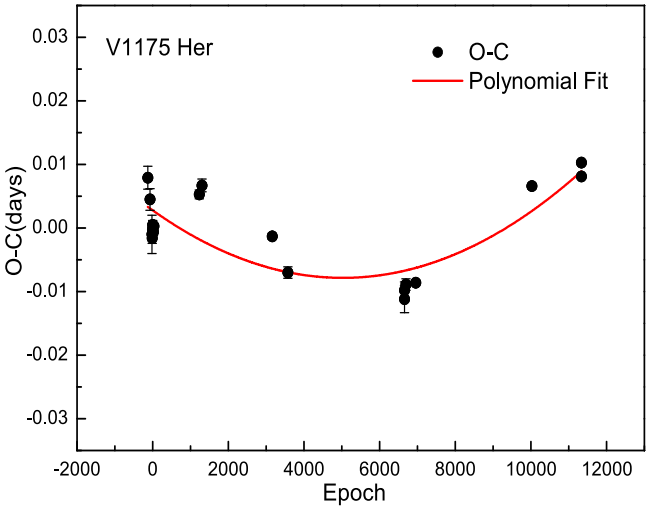

Figure 3. Variation plot of the $(O–C)_I$ vs. Epoch relationship of V1175 Her. The black circles are the CCD photometrically derived $O–C$ values and the red solid line is our polynomial fitting.

period of V1175 Her is increasing. According to Hoffman et al. (2006) this can be explained by mass-transfer from the less massive to the more massive component. So, we decided to add a hot spot on the secondary component and plot the fitting residuals Σ–q relations. In the first panel of Figure 4, it can be observed that the most likely mass ratio of V1175 Her is 4.0.

For V1175 Her, after several iterations and once all the adjustable parameters have converged, we obtained the resultant orbital and spot parameters. These parameters and their corresponding uncertainties obtained from WD calculations are shown in Table 4. Best fits and observed LCs are shown in Figure 5, corresponding to a model including a binary star and a hot spot at 0.25 phase (left panel) and 0.75 (right panel) phase. The proposed geometric configurations for our studied systems, at 0.25 and 0.75 phases, are shown in Figure 6.

Here we take into account our derived photometric solution. Orbital parameters were fixed while fitting this LC and only luminosity and starspot parameters were adjusted. The reason for adjusting the luminosity parameters is due to the fact that the comparison stars used in these two observations are different. The reason for adjusting starspot parameters is that the starspot activity is an important factor affecting the asymmetry of the LCs. A similar method was used to fit the asymmetric LCs of XY Uma (Pribulla et al. 2001) and DV Psc (Pi et al. 2014). The spot parameters were adjusted until the theoretical curve was consistent with the observational results. Our fitting results indicate the presence of a hot spot on the secondary component. The longitude of the hot spot (ϕ_{spot})[14] is found to be 240°.6, its temperature 5772.5 K and its angular radius 18°.3. The best-fit solutions are plotted in Figure 5 and the corresponding geometric configurations are plotted in Figure 6.

For NSVS 2669503, there are no period or high-resolution spectral analyses available. It was not certain if there were hot, or cool, spots on the primary and/or secondary components. After comparing the fitting residuals Σ for four possible scenarios: Case (1) a hot spot (phase $\sim$ 0.75) on the primary component; Case (2) a hot spot (phase $\sim$ 0.75) on the secondary component; Case (3) a cool spot (phase $\sim$ 0.25) on the primary component; and Case (4) a cool spot (phase about 0.25) on the secondary component. After comparing the proposed scenarios (see Table 4), we found that the best-fitting scenario is number 2. For J1334, the resultant photometric solutions are listed in Table 4.

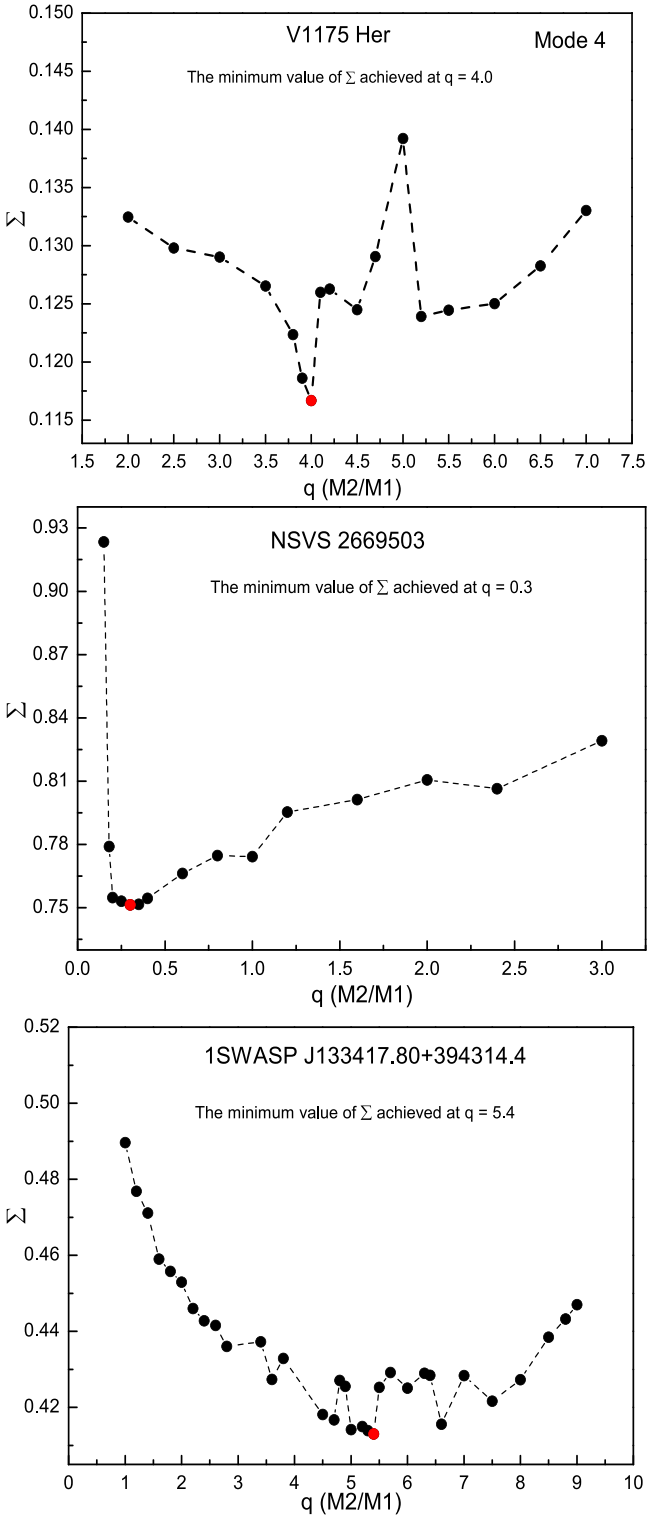

Figure 4. The Σ–q relations derived for each of the three eclipsing binary systems. Vertical axes are the fitted residual values. For V1175 Her, the Σ–q relation was obtained the WD program in Mode 4 (semi-contact binary). This relations are derived adding a hot spot on the secondary component. For NSVS 2669503 and J1334, the Σ–q relation was derived using Mode 3 (contact binary).

[14] The spot longitude (ϕ_{spot}) is in the WD notation and is measured counter-clockwise (as view from above the $+Z$ axis) from the line of star center from 0° to 360°.

Table 4
Theoretical (Fitted) Orbital Parameters of V1175 Her, NSVS 2669503, and J1334

Parameters	V1175 Her (Mode 4[a])	NSVS 2669503 (Mode 3[b])				J1334 (Mode 3[b])
		Case 1[c]	Case 2[d]	Case 3[e]	Case 4[f]	
(1)	(2)	(3)	(4)	(5)	(6)	(7)
q	4.013 ± 0.002	0.300 ± 0.004	0.300 ± 0.004	0.300 ± 0.004	0.300 ± 0.004	5.400 ± 0.005
T_1(K)[g]	5362	4571	4571	4571	4571	4872
T_2(K)	5253 ± 4	4500 ± 5	4471 ± 9	4537 ± 3	4550 ± 1	4775 ± 1
i(∘)	54.751 ± 0.017	71.495 ± 0.140	71.643 ± 0.006	71.725 ± 0.083	71.548 ± 0.046	67.943 ± 0.053
Ω_{in}	7.912	2.466	2.466	2.466	2.466	9.655
Ω_{out}	7.281	2.279	2.279	2.279	2.279	9.015
Ω_1	…	2.467 ± 0.001	2.464 ± 0.001	2.457 ± 0.001	2.458 ± 0.001	9.519 ± 0.004
Ω_2	8.045 ± 0.005	2.467 ± 0.001	2.464 ± 0.001	2.457 ± 0.001	2.458 ± 0.001	9.519 ± 0.004
f	…	…	1.070 (± 0.002)%	4.813 (± 0.002)%	4.278 (± 0.002)%	21.250 (± 0.005)%
$L_1/(L_1+L_2)[U]$	0.269 ± 0.007	0.778 ± 0.036	0.792 ± 0.009	0.759 ± 0.017	0.753 ± 0.008	…
$L_1/(L_1+L_2)[B]$	0.255 ± 0.004	0.769 ± 0.045	0.779 ± 0.017	0.755 ± 0.024	0.751 ± 0.014	0.204 ± 0.002
$L_1/(L_1+L_2)[V]$	0.237 ± 0.003	0.759 ± 0.047	0.767 ± 0.029	0.747 ± 0.025	0.744 ± 0.017	0.194 ± 0.001
$L_1/(L_1+L_2)[R]$	0.235 ± 0.002	0.757 ± 0.045	0.763 ± 0.035	0.748 ± 0.028	0.745 ± 0.022	0.191 ± 0.002
$L_1/(L_1+L_2)$[I]	0.235 ± 0.002	0.758 ± 04288	0.762 ± 0.046	0.750 ± 0.028	0.748 ± 0.025	…
r_1(pole)	0.248 ± 0.058	0.456 ± 0.203	0.456 ± 0.204	0.458 ± 0.205	0.458 ± 0.205	0.235 ± 0.052
r_1(point)	–	0.611 ± 0.378	…	…	…	…
r_1(side)	0.258 ± 0.068	0.490 ± 0.274	0.491 ± 0.276	0.493 ± 0.279	0.492 ± 0.278	0.245 ± 0.062
r_1(back)	0.291 ± 0.111	0.515 ± 0.340	0.516 ± 0.343	0.518 ± 0.347	0.518 ± 0.347	0.284 ± 0.118
r_1(mean)	0.266 ± 0.079	0.518 ± 0.299	0.488 ± 0.274	0.490 ± 0.277	0.489 ± 0.277	0.254 ± 0.077
r_2(pole)	0.464 ± 0.053	0.261 ± 0.215	0.262 ± 0.217	0.263 ± 0.219	0.263 ± 0.218	0.499 ± 0.045
r_2(point)	0.583 ± 0.040	0.369 ± 0.305	…	…	…	–
r_2(side)	0.500 ± 0.072	0.272 ± 0.252	0.273 ± 0.254	0.274 ± 0.258	0.274 ± 0.257	0.546 ± 0.067
r_2(back)	0.522 ± 0.087	0.304 ± 0.410	0.306 ± 0.416	0.308 ± 0.428	0.308 ± 0.427	0.570 ± 0.081
r_2(mean)	0.517 ± 0.063	0.302 ± 0.296	0.280 ± 0.296	0.282 ± 0.302	0.282 ± 0.301	0.538 ± 0.064
Latitude(∘)[g]	90	90	90	90	90	…
Longitude(∘)	160.983 ± 0.145	270.772 ± 0.214	303.376 ± 0.223	69.891 ± 0.254	60.971 ± 0.135	…
Angular radius(∘)	15.289 ± 0.104	7.001 ± 0.142	12.811 ± 0.124	10.783 ± 0.105	18.370 ± 0.259	…
Temperature(K)	5533.510 ± 0.216	5157.54 ± 0.236	5471.47567 ± 0.206	3584.956 ± 0.217	3479.613 ± 0.145	…
$\sum$	0.10504	0.59522	0.40896	0.57123	0.57181	0.41302

Notes.
[a] Mode 4: Semi-contact binary.
[b] Mode 3: Contact binary.
[c] Hot spot (phase about 0.75) on the primary component.
[d] Hot spot (phase about 0.75) on the secondary component.
[e] Cool spot (phase about 0.25) on the primary component.
[f] Cool spot (phase about 0.25) on the secondary component.
[g] Parameters not adjusted in the photometric solution (see Section 4).

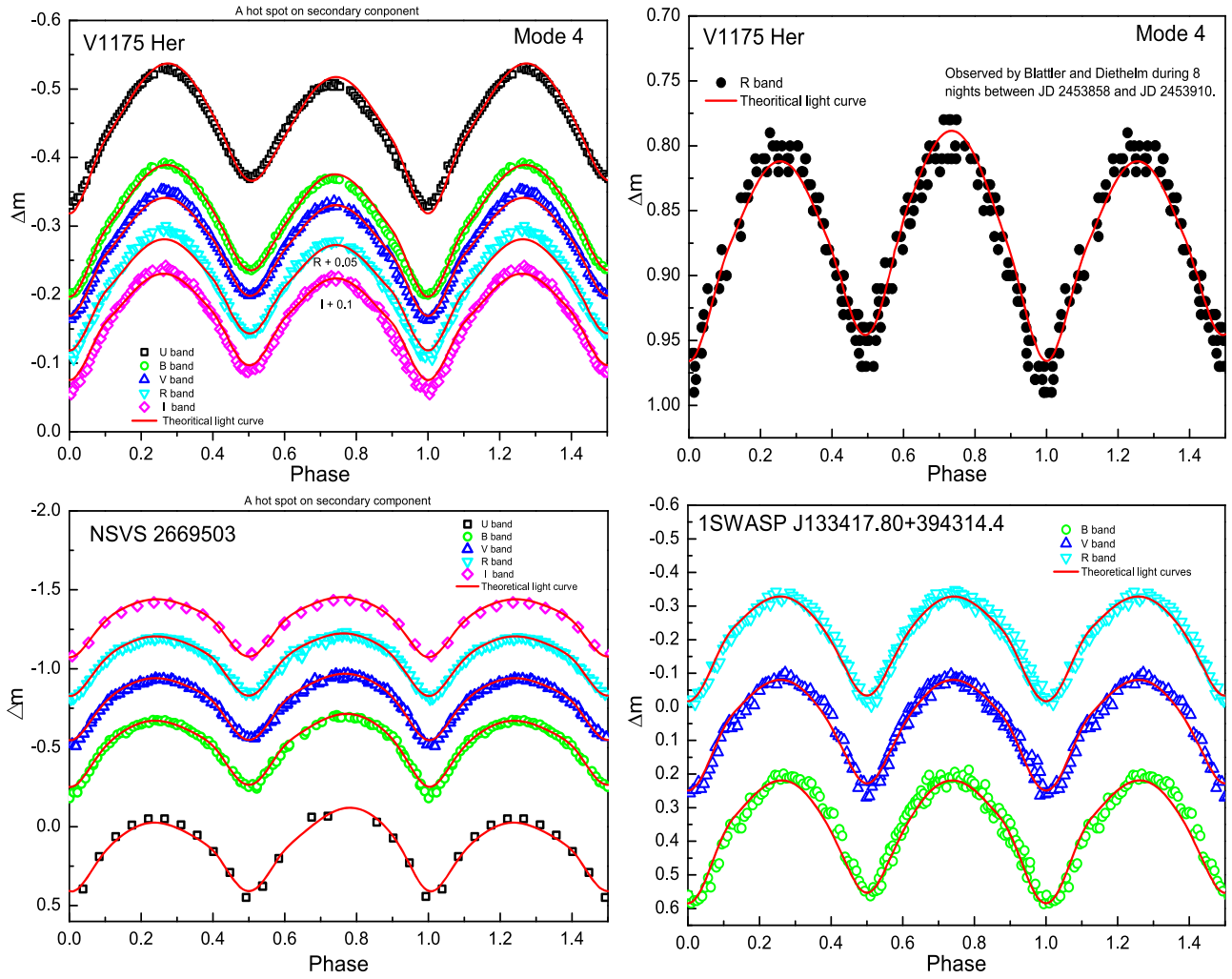

Figure 5. Observational LCs of V1175 Her, NSVS 2669503 and J1334 along with their corresponding theoretical fits. The top two figures are V1175 Her, for which all fittings were made considering Mode 4 (semi-contact binary). In the top-left figure, our observed LCs are shown along with their theoretical fittings. The top-right figure shows the LC obtained by Blättler & Diethelm (2007) but with our derived fitting curve superposed. The bottom two figures are NSVS 2669503 (left) and J1334 (right), both fitted assuming Mode 3 (contact binary) with the WD program.

The observed and theoretical (best-fit solutions) LCs of the three binary systems studied in this paper are plotted in Figure 5. Additionally, our proposed model geometric configurations are shown in Figure 6.

5. Spectral Analysis

By analyzing our low-resolution optical spectra of V1175 Her and NSVS 2669503, which are empirical observations of unresolved light from both components of the system, we classified their joint spectral types using the Hammer program (Covey et al. 2007; West et al. 2011). This program allows us to visually inspect and assign spectroscopical types to the studied objects. Using this method, the joint spectrum of V1175 Her was classified as G7V (±2 subtypes). The corresponding $T_{\rm eff}$ of this spectral type is about 5393 K (Cox 2000), which is very similar to the effective temperatures of the primary component (5362 K) and secondary component (5253 K) deduced by the WD program for V1175 Her. As a result of the lack of high-resolution spectra available, we could not provide the spectral type of each component of V1175 Her. In addition, the presence of Hα(6563 Å) emission is considered to be a primary indicator of chromospheric activity (e.g., Hall 2008). However, a normalized low-resolution spectrum of V1175 Her, shown in Figure 7 (left panel), does not show strong Hα emission.

According to the classification obtained with the Hammer program, the joint spectral type of NSVS 2669503 is K4V (±2 subtypes) and its corresponding $T_{\rm eff}$ is about 4550 K (Cox 2000). This value is also close to the $T_{\rm eff}$ of the primary component (4571 K) and secondary component (4471 K) of NSVS 2669503 estimated using the WD program. The normalized spectrum of NSVS 2669503 is shown in Figure 7 (right panel). No obvious Hα emission line is observed in this spectrum.

6. Discussion and Conclusions

The new multi-band CCD photometric LCs of three eclipsing binary stars (V1175 Her, NSVS 2669503, and J1334) are presented. We also obtained their corresponding photometric solutions using WD. In this section, we discuss their photometric solutions, absolute parameters and evolutionary stages, as well as an interpretation of V1175 Her orbital period variation.

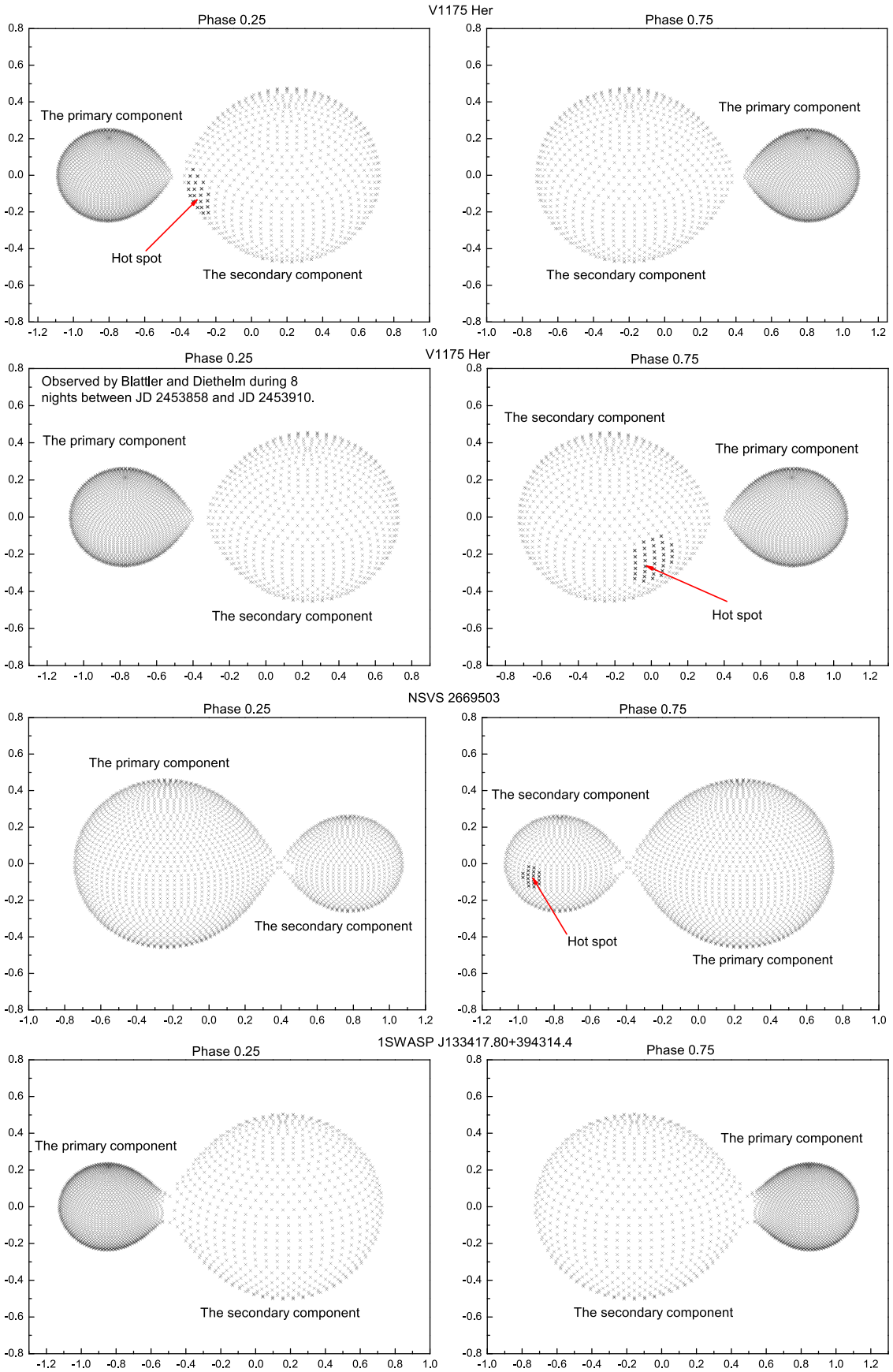

Figure 6. The geometric configurations of V1175 Her, NSVS 2669503 and J1334 in the 0.25 (left) and 0.75 (right) phase, respectively. In these figures, the horizontal axis represents the line perpendicular to the line of sight in orbital plane of the eclipsing binary system and the vertical axis represents the normal direction of the orbital plane of the eclipsing binary system. The units of both axes are the orbital separation of the mass center of the primary and secondary components.

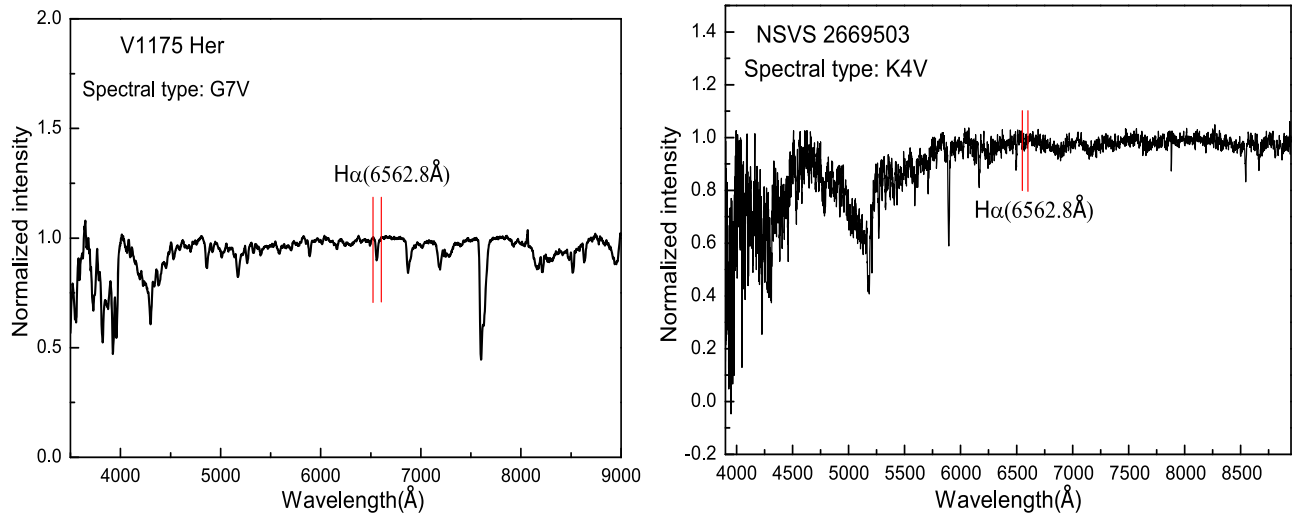

Figure 7. Normalized spectra for V1175 Her (left) and NSVS 2669503 (right). Red marks point the position of the Hα line. The unit of y-axis is the spectral intensity normalized by the source flux density.

6.1. Photometric Solution Analysis

The photometric solution of V1175 Her indicates the source to be a semi-detached binary system with the primary component filling its limiting Roche lobe. The O'Connell effect on the LCs of V1175 Her observed in Blättler & Diethelm (2007) and in this work were satisfactorily fitted (see Figure 5) by adding a hot spot on the secondary component. The longitude, angular radius, and temperature of the hot spot added to the LCs we observed are different from those of the hot spot added to the LCs observed by Blättler & Diethelm (2007). This suggests the presence of starspot activity on the the secondary component of V1175 Her. The resultant orbital parameters show a temperature difference, $\Delta(T_1–T_2)$, of 109 K between both components. In the case of V1175 Her, the ratios of the primary component luminosity to the total luminosity for each of the $UBVRI_C$ bands are: 0.269 ± 0.007 in band-U, 0.255 ± 0.004 in band-B, 0.237 ± 0.003 in band-V, 0.235 ± 0.002 in band-R and 0.235 ± 0.002 in band-I_C.

Based on our photometric solution for NSVS 2669503, we determined that this system is a contact binary. This result is in agreement with the classification derived by Drake et al. (2014). Taking into account the O'Connell effect, we additionally accounted for a hot spot on the secondary component into our calculations. Under this assumption, an acceptable fitting of the LCs is achieved. From the resultant photometric solution, we found that the temperature of the primary component is 100 K hotter than the secondary component. We derived a mass ratio (M_2/M_1) of 0.3, indicating the mass of the primary component to be larger. This indicates that NSVS 2669503 is a type-A W UMa binary (Binnendijk 1970). The ratios of the primary component luminosity to the total luminosity of NSVS 2669503 in each of the $UBVRI_C$ bands are: 0.792 ± 0.009 in band-U, 0.779 ± 0.017 in band-B, 0.767 ± 0.029 in band-V, 0.763 ± 0.035 in band-R and 0.762 ± 0.046 in band-I_C. Moreover, the dimensionless potentials of their components are $\Omega_1 = \Omega_2 = 2.464 \pm 0.001$ with corresponding $\Omega_{in} = 2.466$ and $\Omega_{out} = 2.279$. The contact factor (f) of NSVS 2669503 can be deduced assuming $f = (\Omega_{in} - \Omega_1)/(\Omega_{in} - \Omega_{out})$. This gives $f = 1.070 \pm 0.002\%$.

Our photometric solution for J1334 shows that this is also a contact binary star, in agreement with the result derived by Palaversa et al. (2013). The photometric solution we derived suggests a $\Delta(T_1–T_2) = 97$ K and a mass ratio 5.4. These quantities indicate that J1334 is a type-W W UMa binary (Binnendijk 1970). The primary component luminosity to the total luminosity ratios of J1334 for each of the $UBVRI_C$ bands are: 0.204 ± 0.002 in band-B, 0.194 ± 0.001 in band-V and 0.191 ± 0.002 in band-R. The dimensionless potentials are $\Omega_1 = \Omega_2 = 9.519 \pm 0.004$ with corresponding $\Omega_{in} = 9.655$ and $\Omega_{out} = 9.015$. Therefore, the derived f value for J1334 is $21.250 \pm 0.005\%$.

Table 5
Absolute Parameters of V1175 Her, NSVS 2669503, and J1334

Parameter (1)	V1175 Her (2)	NSVS 2669503 (3)	J1334 (4)
Joint spectral type	G7V ($\pm$ 2)	K4V ($\pm$ 2)	K2V ($\pm$ 2)
$M_1(M_\odot)$	0.87 ($\pm$ 0.05)	0.69 ($\pm$ 0.05)	0.74 ($\pm$ 0.06)
$M_2(M_\odot)$	3.49 ($\pm$ 0.05)	0.21 ($\pm$ 0.05)	4.00 ($\pm$ 0.06)
$a(R_\odot)$	3.23 ($\pm$ 0.08)	1.54 ($\pm$ 0.06)	2.63 ($\pm$ 0.09)
$R_1(R_\odot)$	0.86 ($\pm$ 0.09)	0.75 ($\pm$ 0.07)	0.67 ($\pm$ 0.09)
$R_2(R_\odot)$	1.67 ($\pm$ 0.09)	0.43 ($\pm$ 0.07)	1.42 ($\pm$ 0.09)
$L_1(L_\odot)$	0.54 ($\pm$ 0.05)	0.22 ($\pm$ 0.05)	0.23 ($\pm$ 0.05)
$L_2(L_\odot)$	1.90 ($\pm$ 0.06)	0.07 ($\pm$ 0.06)	0.94 ($\pm$ 0.06)

6.2. Absolute Parameters and Evolutionary Stages

Based on spectral analysis, we found that V1175 Her is a G7V ($\pm$2 subtypes) and NSVS 2669503 is a K4V ($\pm$2 subtypes). The mass of the primary component can be estimated assuming that it follows the Cox relation (Cox 2000). Thus, the derived primary component masses are $M_1 = 0.87 \pm 0.05\ M_\odot$ and $M_1 = 0.69 \pm 0.05\ M_\odot$, for V1175 Her and NSVS 2669503, respectively. Although there was no available spectrum of J1334, considering its primary component effective temperature (4872 ± 155 K), we estimated that J1334 is K2V ($\pm$2 subtypes) and a corresponding primary component mass of $M_1 = 0.74 \pm 0.06\ M_\odot$ (see Cox 2000). The secondary component masses of V1175 Her, NSVS 2669503, and J1334 are $3.49 \pm 0.05\ M_\odot$, $0.21 \pm 0.05\ M_\odot$ and $4.00 \pm 0.06\ M_\odot$, respectively, according to the q ratios from the above photometric solutions.

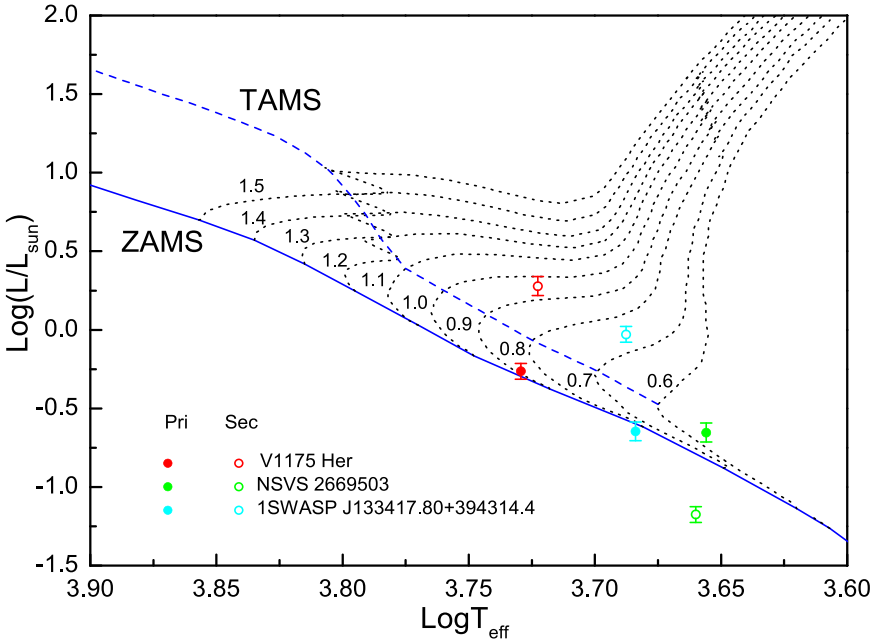

Figure 8. Loci of both components of the three eclipsing binary systems in the log $T_{\rm eff}$–log $(L/L_{\odot})$ diagram. Solid circles are for the primary (pri) components while empty circles are for secondaries (sec). Each binary system is represented by a different color.

Using Kepler's third law ($M_1 + M_2 = 0.0134a^3/p^2$), we calculated the semimajor axis of our three objects, given that a is the semimajor axis in $R_{\odot}$, M_1 in $M_{\odot}$ and p in days. Also, by combining with the mean fractional radii of each component in the photometric solutions, the corresponding radii of the components could be calculated using $R_{1,2} = a \times r_{1,2(\rm mean)}$. Finally, through the equation $L_{1,2} = (R_{1,2}/R_{\odot})^2(T_{1,2}/T_{\odot})^4$, where $T_{\odot} = 5780$ K, the luminosity of each component was derived. The complete set of derived absolute parameters of the analyzed systems is shown in Table 5.

In order to estimate the evolutionary stages of both primary and secondary components of the three eclipsing binary systems, we made a log $(T_{\rm eff})$ − log $(L/L_{\odot})$ diagram (see Figure 8). This diagram includes the zero-age main sequence (ZAMS), the terminal-age main sequence (TAMS), and the evolutionary tracks for solar chemical compositions assuming $Z = 0.019$ and $Y = 0.273$ (Girardi et al. 2000). In Figure 8, the primary components of V1175 Her and J1334 are located near the ZAMS line suggesting that the primary components of these two eclipsing binary systems are MS stars. The primary component of NSVS 2669503 is located between the ZAMS line and the TAMS line, indicating that this component is an evolved MS star. The secondary components of V1175 Her and J1334 lie above the TAMS line, allowing us to infer that the secondary component of V1175 Her might be a G8V type sub-giant with mass 3.49 $M_{\odot}$ and that the secondary component of J1334 might be a K2V type sub-giant with mass 4.00 $M_{\odot}$. The secondary component of NSVS 2669503 lies below the ZAMS line, it can be inferred that such a component is associated to a dwarf star with mass 0.21 $M_{\odot}$. Again considering the relationship between the stellar mass and spectral type (Cox 2000), it can be concluded that this component is of an M5 type. In addition, we plot the solar metallicity isochrones in the log $(T_{\rm eff})$–log $(L/L_{\odot})$ plane (see Figure 9). In Figure 9, the multiple colored dotted lines represent the 0.01, 0.015, 0.03, 0.04, 0.05, and 10 Gyr theoretical isochrones from Baraffe et al. (2015), respectively. As shown in Figure 9, the primary component of V1175 Her is near the 0.05 Gyr isochrone and its secondary component is near the 0.010 Gyr isochrone. This indicates that the age of the primary component of V1175 Her is about 50 Myr and that the age of the secondary component is about 10 Myr. For J1334, the primary component is near the 0.04 Gyr isochrone and the secondary component is not far below the 10 Gyr isochrone. We estimated that the age of the primary component is about 40 Myr and the age of the secondary component is larger than 10 Gyr. For NSVS 2669503, the secondary component is near the 0.05 Gyr isochrone, indicating an age of ∼50 Myr. The primary component is located below the 10 Gyr isochrone. Since there is no corresponding isochrone in the vicinity of this point, we cannot estimate its age, but we can infer that the age of the star is much larger than 10 Gyr.

6.3. Interpretation of Orbital Period Variation

After updating the ephemeris of V1175 Her, we found that there is an obvious upward parabolic trend on its $(O–C)$I versus E diagram, meaning that the orbital period is increasing. After some calculation, we found that its period increases at a rate of $(+3.1 \pm 0.1) \times 10^{-7}$ days yr^{-1}. This phenomenon could be explained by mass-transfer from the less the more massive component (see Hoffman et al. 2006) or by magnetic activity (e.g., Applegate 1992; Lanza et al. 1998). From the photometric solution of V1175 Her, we know that the orbital period increase may be attributed to a mass-transfer effect. According to Singh & Chaubey (1986), the mass-transfer of this eclipsing binary system can be derived with the equation

$$\frac{dP/dt}{P} = 3\left(1 - \frac{M_2}{M_1}\right)\frac{dM_1/dt}{M_1}. \quad (6)$$

Using the derived absolute parameter results of V1175 Her, we estimated a mass-transfer rate of $dM_1/dt = -0.93 \times 10^7\, M_{\odot}$ yr^{-1}. This mass-transfer phenomenon is reported in many EW-type eclipsing binaries, such as HH Uma (Han et al. 2014), V409 Hya (Na et al. 2014), and FZ Ori

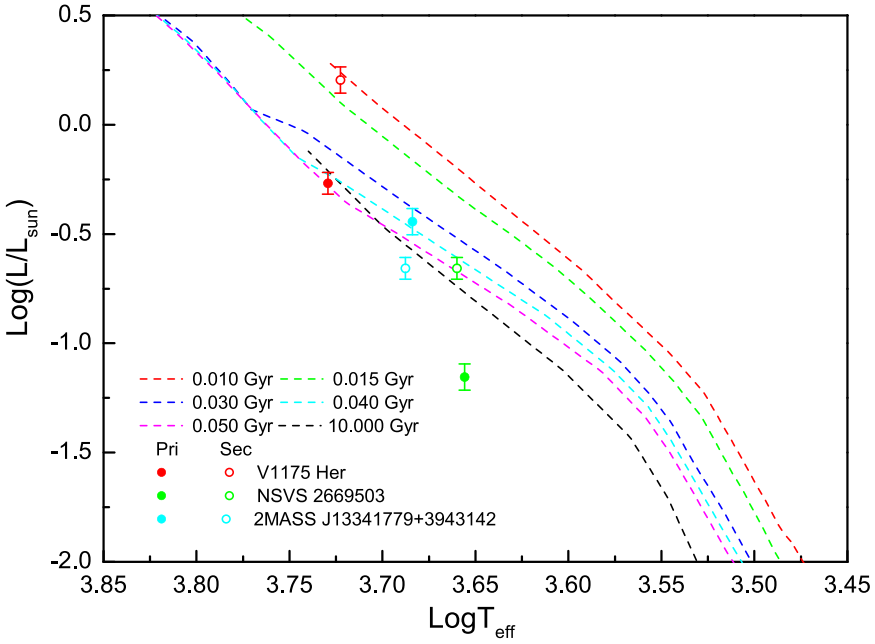

Figure 9. Isochrones of the solar chemical composition (Baraffe et al. 2015) in the log $T_{\rm eff}$–log $(L/L_{\odot})$ diagram. Each isochrone and each binary system are represented in a different color. Solid circles are for primary (pri) components and empty circles for the secondary (sec) components; different colors were used for each binary system.

Table 6
EW-type Binaries (Period <0.5 days) with Mass-transfer Similar to V1175 Her

Name (1)	P(days) (2)	q (3)	Configuration (4)	dP/dt (days yr^{-1}) (5)	$dM/dt(M_{\odot}$ yr$^{-1})$ (6)	References (7)
LO Com	0.28636058	2.478	Contact	-1.180×10^{-7}	0.90×10^{-7}	(1)
V532 Mon	0.4669751997	0.2556	Contact	-1.716×10^{-7}	0.90×10^{-7}	(2)
LP UMa	0.309898	0.331	Contact	$+1.080 \times 10^{-6}$	5.20×10^{-7}	(3)
NGC 7789	0.3917	3.848	Contact	$+2.480 \times 10^{-6}$	2.90×10^{-7}	(4)
V1128 Tau	0.305371	0.534	Contact	-3.460×10^{-8}	1.13×10^{-7}	(5)
FZ Ori	0.399986	0.86	Contact	-2.170×10^{-7}	1.36×10^{-7}	(6)
HH UMa	0.3754937	3.344	Contact	$+2.840 \times 10^{-7}$	1.45×10^{-7}	(7)
V409 Hya	0.472274	0.2155	Contact	$+5.410 \times 10^{-7}$	1.62×10^{-7}	(8)
NGC 6397 V7	0.269861	2.690	Contact	$+4.071 \times 10^{-8}$	2.14×10^{-8}	(9)
NGC 6397 V8	0.271243	0.159	Contact	$+2.569 \times 10^{-7}$	5.22×10^{-8}	(9)
EP And	0.40410869	2.68459	Contact	$+5.220 \times 10^{-8}$	2.81×10^{-8}	(10)
V441 Lac	0.30891501	0.093	Semi-detached	$+5.90 \times 10^{-7}$	1.187×10^{-7}	(11)
V1175 Her	0.32120004	4.0	Semi-detached	$+3.10 \times 10^{-7}$	0.93×10^{-7}	(12)

References. (1) Zhang et al. (2016), (2) He et al. (2016), (3) Guo et al. (2016), (4) Qian et al. (2015), (5) Caliskan et al. (2014), (6) Prasad et al. (2014), (7) Han et al. (2014), (8) Na et al. (2014), (9) Li & Qian (2013), (10) Liao et al. (2013), (11) Li et al. (2016), (12) This paper.

(Prasad et al. 2014). In order to compare V1175 Her with other EW-type eclipsing binaries (period <0.5 days) with similar phenomena, we collected the physical parameters (i.e., period (P), mass ratio (q), configuration, period variation rate (dP/dt), and mass-transfer rate (dM/dt)) for some data available mass-transferred eclipsing binaries. The results are listed in Table 6. From this table, it can be seen that most of these eclipsing binaries have contact configurations, but V441 Lac and V1175 Her are semi-detached, making V1175 Her an interesting research target. In general, the configuration of EW-type systems is contact-type. However, the WD solution shows that V1175 Her is a semi-detached eclipsing binary. This makes V1175 Her a special eclipsing binary system such as V441 Lac (Wang et al. 2015; Li et al. 2016). The formation and evolution of such systems is a topic of future work. A plausible formation and evolution scenario of such eclipsing binary systems is: originating as a W-subtype lightly connected system, with the less massive component is transferring mass to the more massive component. With the mass-transfer, the degree of contact between the two components decreases until the system evolves into a semi-connected system as predicted by the Thermal Relaxation Oscillation models (Lucy 1967). For NSVS 2669503 and J1334, since there was not enough available light minima times, we could not analyze their orbital period, until such observations are carried out.

We appreciate the help given by Peter Boorman in improving the drafting of this document. We also thank the anonymous referee for their helpful comments that contributed to enhance this work. In addition, we are grateful to LAMOST

Spectra Sky Survey for providing us with a spectrum. Guoshoujing Telescope (the Large Sky Area Multi-Object Fiber Spectroscopic Telescope, LAMOST) is a National Major Scientific Project built by the Chinese Academy of Sciences. Funding for the project has been provided by the National Development and Reform Commission. LAMOST is operated and managed by the National Astronomical Observatories, Chinese Academy of Sciences. This research is supported by the UNAM under DGAPA grant PAPIIT IN 105115, and the Joint Fund of Astronomy of the NSFC and CAS grant Nos. U1631236 and U1431114. This work was also supported by the Guizhou Province Office of Education (grant No. 2014298).

ORCID iDs

Raul Michel https://orcid.org/0000-0003-1263-808X
Angel Castro https://orcid.org/0000-0002-7832-5337

References

Akerlof, C., Amrose, S., Balsano, R., et al. 2000, AJ, 119, 1901
Applegate, J. H. 1992, ApJ, 385, 621
Banfi, M., Aceti, P., Arena, C., et al. 2012, IBVS, 6033, 1
Baraffe, I., Homeier, D., Allard, F., et al. 2015, A&A, 577, 42
Binnendijk, L. 1965, VeBam, 27, 36
Binnendijk, L. 1970, VA, 12, 217
Blättler, E., & Diethelm, R. 2007, IBVS, 5799, 1
Butler, C. J., Erkan, N., Budding, E., et al. 2015, MNRAS, 446, 4205
Caliskan, S., Latkovic, O., Djurasevic, G., et al. 2014, AJ, 148, 126
Collier, C. A., Wilson, D. M., West, R. G., et al. 2007, MNRAS, 380, 1230
Covey, K. R., Ivezić, Ž., Schlegel, D., et al. 2007, AJ, 134, 2398
Cox, A. N. 2000, Allen's Astrophysical Quantities (4th ed.; New York: Springer), 388
Cui, X. Q., Zhao, Y. H., Chu, Y. Q., et al. 2012, RAA, 12, 1197
Davidge, T. J., & Milone, E. F. 1984, ApJS, 55, 571
Diethelm, R. 2007, IBVS, 5781, 1
Diethelm, R. 2008, IBVS, 5837, 1
Diethelm, R. 2010, IBVS, 5920, 1
Drake, A. J., Beshore, E., Djorgovski, S. G., et al. 2012, AAS, 219, 428.20
Drake, A. J., Graham, M. J., Djorgovski, S. G., et al. 2014, ApJS, 213, 9
Fan, Y., Bai, J. M., Zhang, J. J., et al. 2015, RAA, 15, 918
Girardi, L., Bressan, A., Bertelli, G., & Chiosi, C. 2000, A&AS, 141, 371
Guo, D. F., Li, K., Hu, S. M., et al. 2016, NewA, 44, 29
Hall, J. C. 2008, LRSP, 5, 2
Han, Q., Li, L., Kong, X., et al. 2014, NewA, 31, 26
He, J. J., Qian, S. B., Soonthornthum, B., et al. 2016, AJ, 152, 120
Hoffman, D. I., Harrison, T. E., McNamara, B. J., et al. 2006, AJ, 132, 2260
Hoffman, D. I., Harrison, T. E., & McNamara, B. J. 2009, AJ, 138, 466
Hoňková, K., Juryšek, J., Lehký, M., et al. 2013, OEJV, 160, 1
Kallrath, J., & Milone, E. F. 1999, Eclipsing Binary Stars: Modeling and Analysis (New York: Springer)
Kwee, K. K., & van Woerden, H. 1956, BAN, 12, 327
Landolt, A. U. 1992, AJ, 104, 340
Landolt, A. U. 2009, AJ, 137, 4186
Lanza, A. F., Rodonó, M., & Rosner, R. 1998, MNRAS, 296, 893
Larson, S., Beshore, E., Hill, R., et al. 2003, DPS, 35, 3604
Li, K., Hu, S. M., Guo, D. F., et al. 2016, JApA, 37, 16
Li, K., & Qian, S. B. 2013, NewA, 25, 12
Liao, W. P., Qian, S. B., Li, K., et al. 2013, AJ, 146, 79
Lohr, M. E., Norton, A. J., Kolb, U. C., et al. 2013, A&A, 549, 86
Lucy, L. B. 1967, ZA, 65, 89
Lucy, L. B. 1968a, ApJ, 151, 1123
Lucy, L. B. 1968b, ApJ, 153, 877
Luo, A. L., Zhang, H. T., Zhao, Y. H., et al. 2012, RAA, 12, 1243
Na, W. W., Qian, S. B., Zhang, L., et al. 2014, NewA, 30, 105
Nelson, R. H. 2007, Software by Bob Nelson, https://www.variablestarssouth.org/software-by-bob-nelson/
Nelson, R. H. 2010, IBVS, 5929, 1
Nelson, R. H. 2016, IBVS, 6164, 1
O'Connell, D. J. K. 1951, MNRAS, 111, 642
Palaversa, L., Ivezić, Ź., Eyer, L., et al. 2013, AJ, 146, 101
Paschke, A., & Brát, L. 2006, OEJV, 23, 13
Pi, Q. F., Zhang, L. Y., Bi, S. L., et al. 2017, AJ, 154, 260
Pi, Q. F., Zhang, L. Y., Li, Z. M., et al. 2014, AJ, 147, 50
Pollacco, D. L., Skillen, I., Collier Cameron, A., et al. 2006, PASP, 118, 1407
Prasad, V., Pandey, J. C., Patel, M. K., et al. 2014, Ap&SS, 353, 575
Pribulla, T., Chochol, D., Heckert, P. A., et al. 2001, A&A, 371, 997
Qian, S. B., Essam, A., Wang, J. J., et al. 2015, AJ, 149, 38
Richards, M. T., Cocking, A. S., Fisher, J. G., et al. 2014, ApJ, 795, 160
Rucinski, S. M. 1973, AcA, 23, 79
Sesar, B., Stuart, J. S., Ivezić, Ž., et al. 2011, AJ, 142, 190
Singh, M., & Chaubey, U. S. 1986, Ap&SS, 124, 389
Skrutskie, M. F., Cutri, R. M., Stiening, M. D., et al. 2006, AJ, 131, 1163
Van Hamme, W. 1993, AJ, 106, 209
Wang, D. M., Zhang, L. Y., Han, X. M., et al. 2015, NewA, 36, 32
Wang, S. G., Su, D. Q., Chu, Y. Q., et al. 1996, ApOpt, 35, 25
West, A. A., Morgan, D. P., Bochanski, J. J., et al. 2011, AJ, 141, 97
Wilson, O. C. 1978, ApJ, 226, 379
Wilson, R. E. 1979, ApJ, 234, 1054
Wilson, R. E. 1990, ApJ, 356, 613
Wilson, R. E. 1994, PASP, 106, 921
Wilson, R. E., & Devinney, E. J. 1971, ApJ, 166, 605
Woźniak, P. R., Vestrand, W. T., Akerlof, C. W., et al. 2004, AJ, 127, 2436
Zhang, L. Y., Lu, H. P., Han, X. M., et al. 2018, NewA, 61, 36
Zhang, L. Y., Yue, Q., Lu, H. P., et al. 2017, RAA, 17, 10
Zhang, Y., Han, Q. W., & Liu, J. Z. 2016, PASP, 128, 4201
Zhao, G., Zhao, Y. H., Chu, Y. Q., Jing, Y. P., & Deng, L. C. 2012, RAA, 12, 723